ARTICLE

OBC
www.rsc.org/obc

Controlling the rate of shuttling motions in [2]rotaxanes by electrostatic interactions: a cation as solvent-tunable brake†

Pradyut Ghosh,‡[a] Guido Federwisch,[a] Michael Kogej,[a] Christoph A. Schalley,*[a] Detlev Haase,[b] Wolfgang Saak,[b] Arne Lützen*[b] and Ruth M. Gschwind*[c]

[a] *Kekulé-Institut für Organische Chemie und Biochemie der Universität, Gerhard-Domagk-Str. 1, D-53121, Bonn, Germany. E-mail: c.schalley@uni-bonn.de; Fax: +49-228-735662; Tel: +49-228-735784*

[b] *Institut für Reine und Angewandte Chemie der Universität, Postfach 2503, D-26111, Oldenburg, Germany. E-mail: arne.luetzen@uni-oldenburg.de; Fax: +49-441-7983329; Tel: +49-441-7983706*

[c] *Institut für Organische Chemie der Universität, Universitätsstr. 31, D-93053, Regensburg, Germany. E-mail: ruth.gschwind@chemie.uni-regensburg.de; Fax: +49-941-9434617; Tel: +49-941-9434625*

Received 13th May 2005, Accepted 17th June 2005
First published as an Advance Article on the web 1st July 2005

A series of rotaxanes, with phenolic axle centerpieces and tetralactam macrocycles as the wheels, has been prepared in good yields. The threaded rotaxane structure is confirmed in the gas phase by tandem mass spectrometric experiments through a detailed fragmentation pattern analysis, in solution by NMR spectroscopy, and in the solid state through X-ray crystallography. A close inspection of the ^{1}H,^{1}H NOESY and ^{1}H,^{1}H ROESY NMR data reveals the wheel to travel along the axle between two degenerate diamide "stations" close to the two stoppers. By deprotonation of a phenolic OH group in the axle centerpiece with Schwesinger's P1 base, surprisingly no additional shuttling station is generated at the axle center, although the wheel could form rather strong hydrogen bonds with the phenolate. Instead, the wheel continues to travel between the two diamide stations. Experimental data from ^{1}H,^{1}H NOESY spectra, together with theoretical calculations, show that strong electrostatic interactions between the phenolate moiety and the P1 cation displace the wheel from the "phenolate station". The cation acts as a "brake" for the shuttling movement. Instead of suppressing the shuttling motion completely, as observed in other rotaxanes, our rotaxane is the first system in which electrostatic interactions modulate the speed of the mechanical motion between a fast and a slow motion state as a response to a reversible external stimulus. By tuning these electrostatic interactions through solvent effects, the rate of movement can be influenced significantly, when for example different amounts of DMSO are added to dichloromethane. Besides the shuttling motion, circumrotation of the wheel around the axle is observed and analyzed by variable temperature NMR spectroscopy. Force field and AM1 calculations are in good agreement with the experimental findings.

Introduction

Since the mid-eighties, different template effects[1,2] have been developed in order to provide facile access to mechanically bound species, among them coordination to a central metal ion,[3] and complex formation through π-donor–π-acceptor interactions,[4] or hydrogen bonding to cations,[5] neutrals,[6] or anions.[7] The synthesis and characterization of molecular machines[8] based on such interlocked molecules is a rapidly growing field in supramolecular chemistry.[9] Mechanically interlocked species combine motional freedom of their parts relative to each other with high stability due to the mechanical bond,[10] so that the control of molecular motion by external stimuli[11] such as pH,[12] light,[13] or electrons[14] is an attractive goal. Many other functional properties have been studied, for example, the electron or energy transfer from one stopper to the other,[15] the quenching of luminescence in self-assembled pseudorotaxanes,[16] the photoswitchability of the catenanes' ring geometry,[17] the electric conductance through poly(rotaxanes)[18] and the implementation of logic functions at the molecular level,[19] just to name a few.

This study utilizes a recently published[20] synthesis for the generation of a series of molecular shuttles based on [2]rotaxanes **1@2**–**1@4** (Scheme 1) which bear a phenolic OH group in the center of their axles. Since the wheels are of the tetralactam type,[21] they are capable of forming hydrogen bonds with the axle.[7,22] Recently, Leigh *et al.*[12] reported a system in which protonation and deprotonation of such an OH group induced the motion of a smaller tetralactam wheel between two different stations along the axle. In the deprotonated state, the wheel is

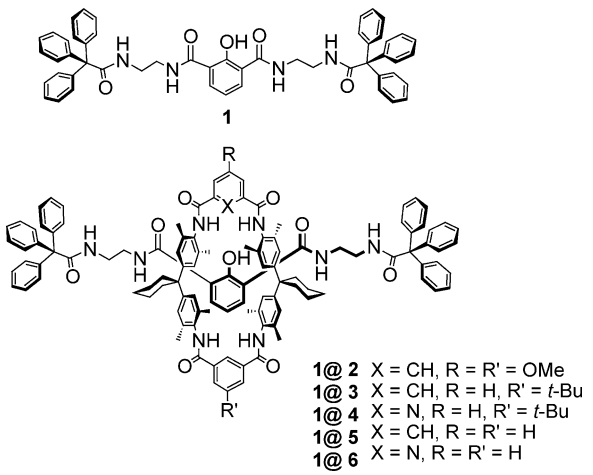

Scheme 1 Structures of rotaxanes **1@2**–**1@6** (**2**–**6** are differently substituted wheels; symmetrical **5** and **6** have been used in the calculations below to reduce the computer time necessary).

† Electronic supplementary information (ESI) available: synthetic protocols, experimental details, theoretical calculations not included in the main text. See http://dx.doi.org/10.1039/b506756a

‡ Present address: *Central Salt & Marine Chemicals Research Institute, G. B. Marg, Bhavnagar, 364002, India.*

DOI: 10.1039/b506756a

located at the phenolate station due to the formation of stronger hydrogen bonds. In contrast, our rotaxanes have symmetrical axles with two identical stations close to the two stoppers that permit degenerate shuttling processes between the two axle ends. Surprisingly, in view of the literature precedent,[23] addition of acids and bases to these rotaxanes does not switch the wheel position between the peripheral diamide and the central phenolate stations, but allows tuning of the shuttling rate of the wheel between the two diamide stations. The novel features of the present rotaxanes are that the speed of wheel shuttling can be switched between "fast" and "slow" by a reversible external stimulus rather than switching it "off" or "on" and that solvent effects provide means to tune the shuttling speed in the "slow-motion" state.

Results and discussion

1. Synthesis and characterization of rotaxane structure

Rotaxanes **1**@**2**–**1**@**4** have been synthesized utilizing the recently published template strategy[20] (for details, see the electronic supplementary information). The threaded topology of these rotaxanes can be unambiguously characterized in the gas phase, in solution, and in the solid state. Thus, three independent pieces of evidence for the rotaxane structure are available:

(i) The negative-mode ESI mass spectra of rotaxane **1**@**4** and a 1 : 1 mixture of axle **1** and wheel **4** (Fig. 1) provide evidence for a rotaxane structure.[24] Ionization of the rotaxane to yield an anion can easily be achieved with this soft ionization technique through deprotonation of the phenol in the axle centerpiece. The spectrum of the rotaxane (Fig. 1, top trace) does not show any signals at the m/z ratios for the deprotonated axle $\mathbf{1}^-$ (m/z = 805) nor the deprotonated wheel $\mathbf{4}^-$ (m/z = 960). In marked contrast, strong signals for axle and wheel are observed under the same conditions, when a sample was analyzed that contained a 1 : 1 mixture of **1** and **4** (bottom trace), which can form the corresponding non-threaded hydrogen-bonded complex $\mathbf{1}^-\cdot\mathbf{4}$. This complex is indeed observed as a minor signal at m/z = 1767. Variations of the ionization conditions significantly affected the relative ratio of this complex ion and the ions corresponding to free axle and wheel, while they had virtually no effect on the spectrum of the rotaxane. Even more conclusive are the negative ion MS/MS spectra[25] shown in Fig. 2. After careful isolation of the monoisotopic rotaxane parent ion $\mathbf{1}^-$@**4** at m/z 1767, argon is introduced into the FT-ICR cell as the collision gas and the ions are subjected to collision-induced dissociation (CID). The rotaxane decomposes by fragmentation of the axle thereby releasing the wheel (top trace). Only a very minor signal is seen for the intact deprotonated axle at m/z = 805, which can be traced back to a significantly more energy-demanding cleavage of the wheel. Rather, fragments of the axle are observed at m/z = 518, 505, and 243, which correspond to the bond cleavages and 1,2-elimination reactions indicated in Fig. 2. Thus, the fragmentation of *covalent bonds* within the axle leads to simultaneous cleavage of the mechanical bond. Again, the axle-wheel complex $\mathbf{1}^-\cdot\mathbf{4}$ formed under identical electrospray ionization conditions and treated exactly the same way as the rotaxane behaves differently. As expected for a *non-covalently hydrogen-bonded species*, wheel **4** is lost in the CID experiment and the negatively charged axle $\mathbf{1}^-$ is formed as the major product at m/z = 805. The consecutive fragmentations of the axle are similar to the fragments observed for the

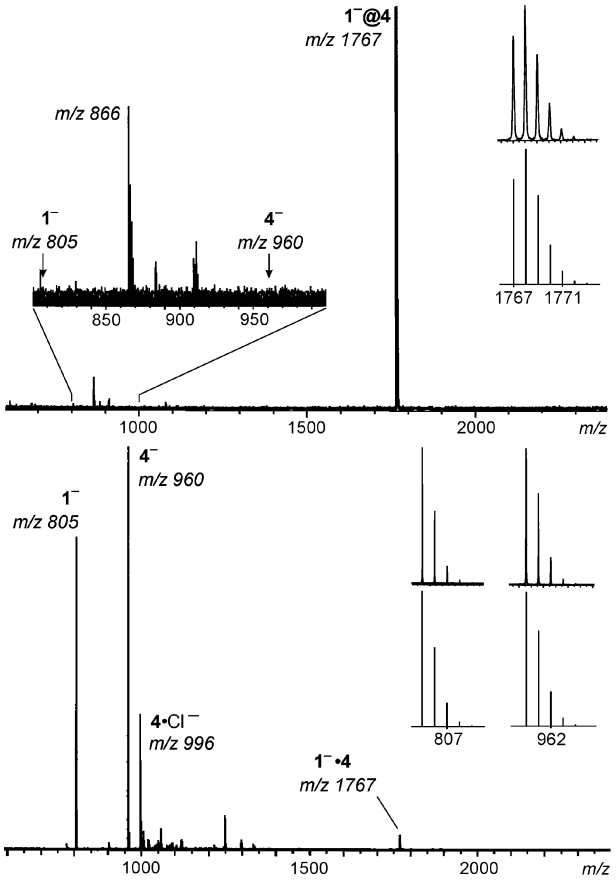

Fig. 1 Negative ion ESI mass spectra of *ca.* 10 μM methanol solutions of rotaxane **1**@**4** (top trace) and a 1 : 1 mixture of its components **1** and **4** (bottom trace). The inset on the left shows the region between m/z = 800 and 1000 in order to demonstrate the absence of significant signals for the rotaxane axle and wheel. The insets on the right compare the experimental isotope patterns (top) with those calculated on the basis of natural abundances (bottom).

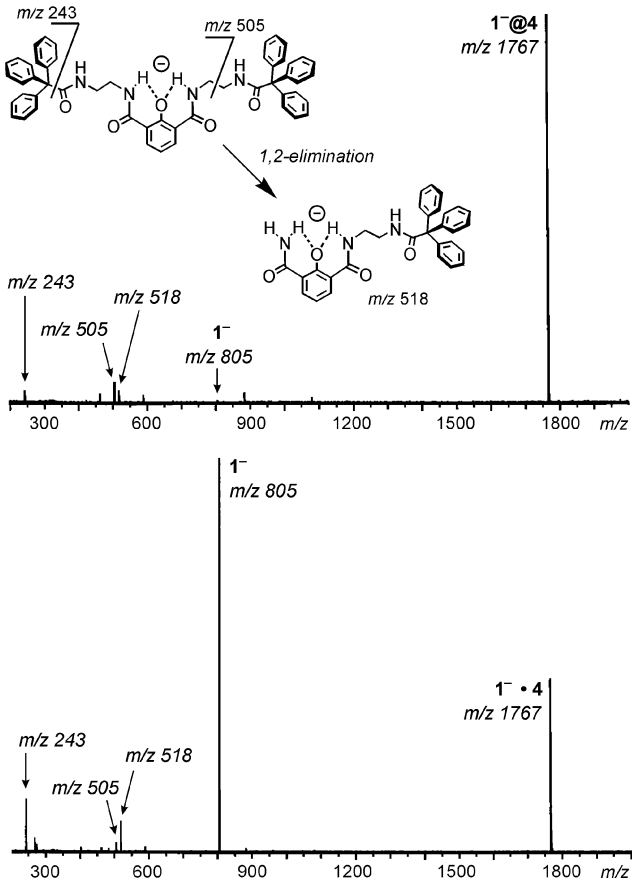

Fig. 2 MS/MS mass spectra of collisionally activated ions $\mathbf{1}^-$@**4** (top) and $\mathbf{1}^-\cdot\mathbf{4}$ (bottom). The inset shows the fragmentation pathways observed for the axle in both spectra between m/z 200 and 550 that lead to the signals at m/z = 243, 505, and 518. The same fragmentations have been found in the collision-induced fragmentations of the deprotonated axle alone.

rotaxane. These experiments confirm the threaded nature of the rotaxane and permit us to distinguish the mechanically bound species from a hydrogen-bonded complex of axle and wheel. The qualitative fragmentation pattern is also in agreement with energetic considerations. While more than two-thirds of the hydrogen-bonded complex of $\mathbf{1}^-$ and **4** has decomposed, the sum of all fragments of the rotaxane amounts to only *ca.* 15% of all signals in the spectrum. This reflects the weaker bond strength of the hydrogen-bonded complex *versus* the strength of the mechanical bond of the rotaxane that requires cleavage of a covalent bond for fragmentation. The other rotaxanes behave similarly so that we refrain from a discussion of their mass spectra here.

(ii) The second piece of evidence comes from crystal structure analysis.§ Suitable single crystals of rotaxane **1@2** were obtained by slowly evaporating dichloromethane from a saturated solution of the rotaxane in a 1 : 1 mixture of dichloromethane and methanol. The Ortep plot (Fig. 3) unambiguously shows the axle to be threaded with one stopper bound on each side of the wheel. The axle center piece bears an in/out conformation (for more details, see below) of the two amide groups next to the phenolate stabilized through an N–H · · · O–H · · · O=C hydrogen bonding pattern (dotted lines in Fig. 3). As confirmed by the NMR data below, the wheel is held on one of the ethylene diamine spacers by a total of four hydrogen bonds. Each isophthalic acid subunit of the wheel is connected to one carbonyl group of the axle by two hydrogen bonds in a forked manner. A–B bond lengths are between 2.96 and 3.33 Å and N–H · · · O angles are between 145 and 165°, values typical for such hydrogen bonds.

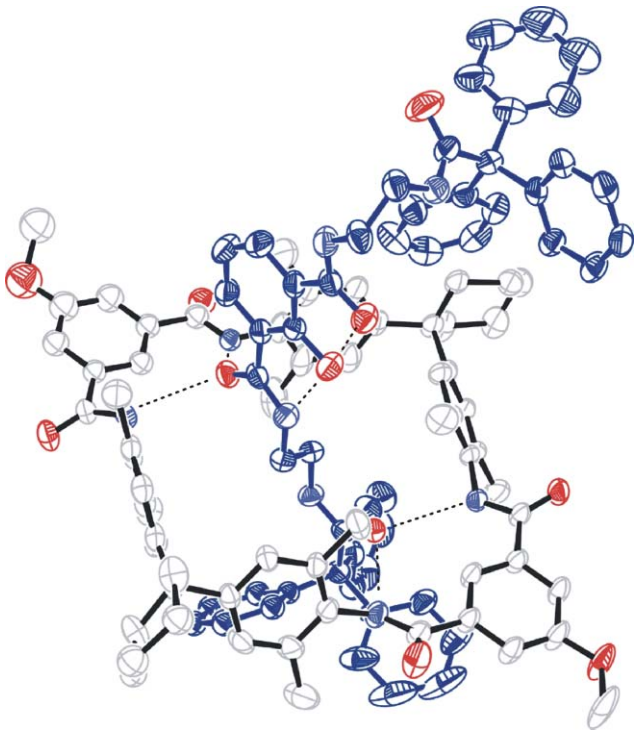

Fig. 3 Ortep plot of the X-ray single crystal structure of rotaxane **1@2**. Blue parts represent the axle, black parts the wheel. The dotted lines indicate hydrogen bonds.

(iii) Evidence for the rotaxane structure in solution is also available from NMR experiments. Fig. 4 compares the ^{1}H-NMR spectra of free wheel **4** (trace a), the rotaxane **1@4** (trace b), the axle **1** (trace c) and a 1 : 1 mixture of axle **1** and wheel **4** (trace d) in DMF-d_7 at 333 K. The mixture of both components only reveals shifts of the amide protons that are likely due to

§ CCDC reference number 230812. See http://dx.doi.org/10.1039/b506756a for crystallographic data in CIF or other electronic format.

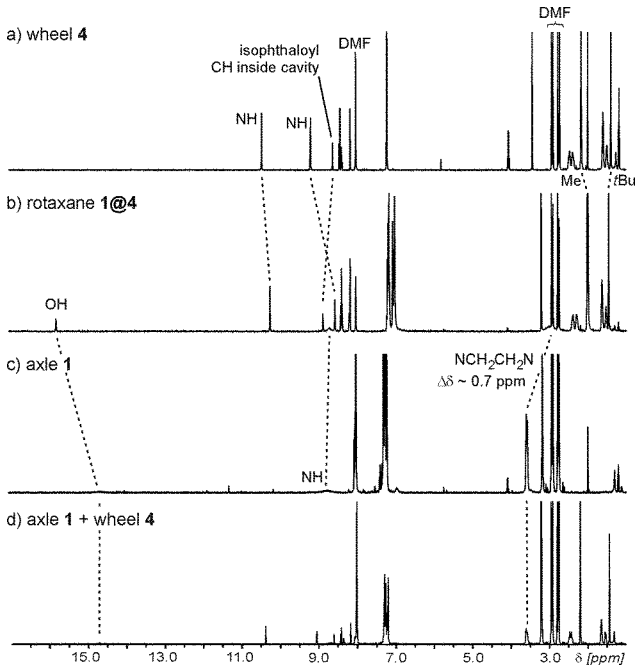

Fig. 4 ^{1}H NMR spectra recorded at 333 K in DMF-d_7 of (a) macrocycle **4**, (b) rotaxane **1@4**, (c) axle **1**, and (d) a 1 : 1 mixture of axle **1** and wheel **4**. For the ease of comparison, the rotaxane spectrum is shown between the spectra of its components. Dotted lines indicate signals which are shifted in the rotaxane spectrum relative to their positions in the spectra of the free components.

changes in hydrogen bonding. Instead, a significant shift ($\Delta\delta$ = 0.8 ppm) and sharpening of the phenol OH signal and smaller shifts of the amide hydrogen atoms of the wheel ($\Delta\delta$ = 0.3 and 0.6 ppm) are observed for the rotaxane relative to their position in the spectra of the free components. Besides these, upfield shifts of carbon-centered hydrogen atoms incorporated in the axle are often found due to the anisotropy of the aromatic rings incorporated in the wheel. Rather large values of up to 1.7 ppm have been recorded.[10] These anisotropy effects are particularly large for those parts of the axle located exactly in the center of the wheel cavity. In the spectrum of **1@4**, the largest upfield shifts are observed for the ethylene diamine spacers in the axle ($\Delta\delta$ = 0.7 ppm) indicating that one of the ethylene diamine units is located inside the wheel cavity as observed in the crystal structure.§ The methylene signals inside the cavity are averaged with those at the other half of the axle due to a motion of the wheel along the axle which is fast on the NMR timescale at 333 K in DMF-d_7. One can estimate the upfield shift for the inside methylene signals to be about twice as large as measured (*ca.* $\Delta\delta$ = 1.4 ppm), when this motion becomes slow on the NMR time scale. That agrees well with the shift differences observed for other rotaxanes earlier[10] and is confirmed by low temperature data discussed below. Also, the wheel's isophthalic acid hydrogen atoms pointing into the cavity experience a small shift, indicating that they are affected by the presence of the axle.

Rotaxane **1@4** bears a pyridine, which renders the wheel unsymmetrical. At 233 K in dichloromethane-d_2, the rotation of the wheel is slow on the NMR timescale, as indicated by the double set of signals (Fig. 5) which correspond to two co-existing conformations. In one of these, the pyridine part is hydrogen bonded to the carbonyl oxygen adjacent to the stopper. In the other one, it is bound to the carbonyl group at the central phenolate. The two signals for the OH group are found in roughly a 1 : 3 ratio around 15.4 ppm. Also, the two amide protons of the wheel adjacent to the pyridine appear as two signals in the same intensity ratio around 10.3 ppm. Consequently, the two orientations of the wheel differ only slightly in energy by *ca.* 2 kJ mol^{-1}.

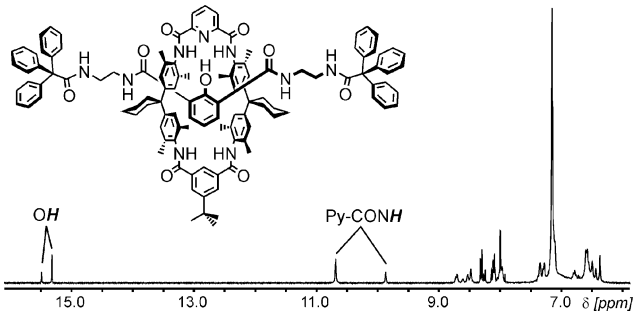

Fig. 5 ^{1}H NMR spectrum of **1**@**4** in CD_2Cl_2 at 233 K. Note that two signals for the OH and NH protons indicate formation of two different conformers which slowly interconvert on the NMR time scale.

The structures of rotaxanes **1**@**2** and **1**$^-$@**2** were investigated in detail in solution. Two main questions arise: (a) Is the structure of **1**@**2** in solution identical to the crystal structure as suggested by the chemical shifts discussed above? (b) Does the deprotonation to **1**$^-$@**2** introduce a different shuttling station and therefore a different structure of the whole rotaxane? To answer these questions and to gain further insight into the structures of **1**@**2** and **1**$^-$@**2** in solution, ^{1}H,^{1}H NOESY and ^{1}H,^{1}H ROESY spectra of both rotaxanes were recorded in dichloromethane-d_2 at 233 K (for the nomenclature used to denote the individual protons in the Figures, see Scheme 2). For the interpretation of the obtained dipolar interactions, the remaining dynamic behaviour of both rotaxanes has to be taken into account (see below). Thus, even at this low temperature, both rotaxanes show a shuttling of the symmetrical wheel along the axle as well as a rotation of the wheel fast relative to the shuttling motion, but slow on the NMR time scale. The dynamic behavior of the rotaxanes together with the fact that the nuclear Overhauser effect strongly overestimates small distances in short time contacts, allow only a qualitative analysis of the NOESY and ROESY spectra.

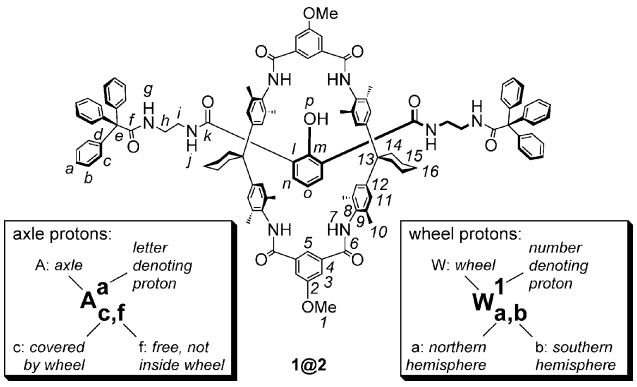

Scheme 2 Nomenclature used for the identification of individual protons. A and W denote the two rotaxane components, superscripts identify the particular proton (letters for axle protons, numbers for wheel protons), and subscripts label the two halves of axle and wheel resulting from desymmetrization of the spectra under slow exchange conditions at lower temperatures.

The crystal structure of **1**@**2**§ is ideal for comparison with the NOE data. A close inspection of the crystal structure shows some main structural characteristics: (a) The wheel is directly positioned over the ethylene spacer of the covered half of the axle. Various NOE cross signals between these methylene protons and the amide protons as well as the aromatic protons of the wheel directed towards the axle confirm this structural feature. (b) A second characteristic of **1**@**2** is the *in*/*out*-conformation of the inner amide NH protons also found in the calculations (see below), with the wheel being positioned on the *in* part of the axle (see Fig. 3). There, the *in* NH proton forms an internal hydrogen bond to the central phenol oxygen and the *in* CO is able to form intermolecular hydrogen bonds to the wheel. A second internal hydrogen bond is formed between the OH group of the phenol and the *out* CO group. This structural feature is confirmed in solution by NOE contacts of the NH protons of the inner amide moieties (Fig. 6).

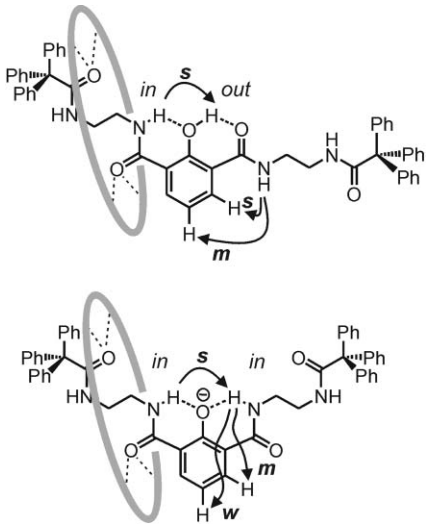

Fig. 6 Selected NOE contacts revealing the reorientation of the two amide groups adjacent to the central axle phenol(ate) in the protonated and deprotonated forms of **1**@**2** (s: strong, m: medium, w: weak contacts).

Furthermore, close interproton contacts between the phenyl stopper of the covered half of the axle and the protons of the wheel are expected from the crystal structure of **1**@**2**. As example of the NOE pattern of these contacts, typical cross peaks of the *ortho*-protons of this stopper are shown in Fig. 7a1 and 7a2. Similar close contacts to the wheel are found for the amide proton next to this stopper (see Fig. 7a3). In all of these spectra, the intensities of the cross peaks between axle and wheel are nearly equally distributed over the exchanging protons in the wheel, *e.g.* the amide protons of the wheel (see Fig. 7a2), indicating the fast rotation of the wheel. In contrast,

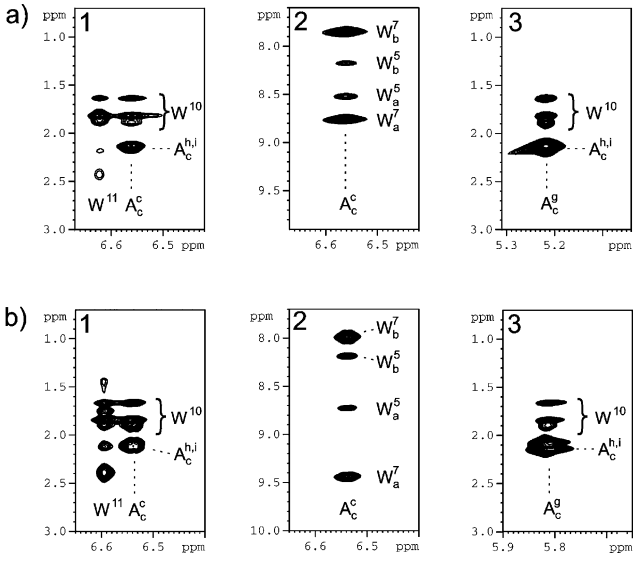

Fig. 7 Sections of ^{1}H,^{1}H NOESY spectra of **1**@**2** (a) and **1**$^-$@**2** (b) at 233 K in mixtures of CD_2Cl_2 and DMSO-d_6. Selected cross signals between the phenyl stopper of the half of the axle covered by the wheel (1 and 2) as well as the amide proton next to this stopper and protons of the wheel (3) show the similarity of the wheel position in **1**@**2** and **1**$^-$@**2** in solution and the crystal structure of **1**@**2**. For the nomenclature applied to distinguish individual protons, see Scheme 2.

the other half of the axle, uncovered by the wheel, as well as the other stopper do not show any dipolar interactions to the wheel (NOESY spectra not shown). In addition to the few discussed characteristics, the whole qualitative NOE pattern of **1@2** is in accordance with its crystal structure. Therefore, a structural similarity between the structure of **1@2** in the solid state and in solution is proposed.

Now, the question needs to be addressed whether the deprotonation to **1**$^-$**@2** introduces a new, better shuttling station and affects the whole structure. For deprotonation, Schwesinger's P1 base[26] was used, because the large, lipophilic cation improves the solubility of the resulting salt even to beyond that of the neutral rotaxane. As expected, the deprotonation leads to a change of the intramolecular hydrogen bonding pattern of the axle from an *in/out* to an *in/in* conformation of the inner amide NH protons (see Fig. 6). This is indicated by a significant low field shift of these NH protons by more than 3 ppm combined with a modified NOE pattern. Now both inner NH protons build hydrogen bonds to the phenolate oxygen. However, slightly different NOE contacts between the two NH protons and the aromatic protons of the phenolate moiety in *meta* position indicate a small twist of the free half of the axle caused by the presence of the P1 base (see below). Beside that and chemical shift deviations of the other NH protons, influenced by the change in pH, the chemical shifts of **1**$^-$**@2** and **1@2** are surprisingly similar (see the supplementary information, Table S1), especially the chemical shifts of the ethylene spacers covered by the wheel, which, although they should be most affected by a different position of the wheel, are nearly identical (Table 1). A further proof for an almost unaltered position of the wheel in **1**$^-$**@2** and **1@2** is given by the comparison of the intermolecular NOE pattern between axle and wheel. No significant differences between their NOE derived interproton contacts are observed. This is exemplarily shown in Fig. 7 for the characteristic NOE cross signals discussed above. Therefore, we conclude that in **1**$^-$**@2** an *in/in* conformation is formed within the axle center piece, but compared to **1@2** the position of the wheel is identical.

Thus, the wheel in **1**$^-$**@2** does not use the phenolate moiety to build hydrogen bridges and no new shuttling station is introduced here as expected from previous work.[12] An explanation supported by experiment involves strong electrostatic interactions between the negative charge at the phenolate moiety and the positive charge of the P1 cation. From the NOESY spectra of **1**$^-$**@2**, dipolar interactions between the base and the free half of the axle are detected. The strongest intermolecular NOEs for the NH proton of the base are observed to the meta position of the phenolate moiety (Fig. 8) and to the protons of the ethylene groups on the uncovered half of the axle. This as well as other NOE cross peaks not discussed in detail indicate that the cation approaches the phenolate moiety from the uncovered side of the axle and pushes the wheel away from the phenolate moiety. Thus, the sum of the electrostatic interactions between the charged moieties and the hydrogen bonds at the diamide station seems to be stronger than the otherwise more favorable hydrogen bridges between the wheel amide groups and the phenolate oxygen. This structural explanation is further confirmed by the theoretical calculations as well as the dynamic behavior discussed below.

Table 1 Chemical shifts of the ethylene protons of **1**$^-$**@2** and **1@2** in a mixture of CD_2Cl_2 and DMSO-d_6 at 233 K

Proton[a]	**1**$^-$**@2** ^{1}H/ppm	**1@2** ^{1}H/ppm
A_c^h	2.13	2.12
A_c^i	2.07	2.10
A_f^h	3.33	3.59
A_f^i	3.40	3.44

[a] For the nomenclature, see Scheme 2.

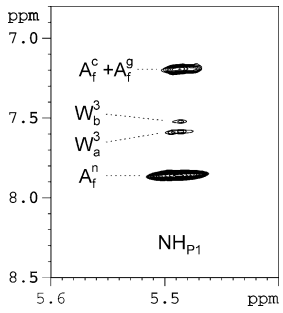

Fig. 8 Section of a ^{1}H,^{1}H NOESY spectrum of **1**$^-$**@2** at 233 K in CD_2Cl_2 and 10% DMSO-d_6 showing dipolar interactions between the NH proton of the P1 cation (NH_{P1}) and protons on the uncovered half of the axle as well as the wheel.

2. Calculations

For the further discussion of the dynamic features, it is advantageous to study the rotaxanes in greater detail by theory, which may complement the experimental results by adding more subtle structural features to the picture. Therefore, AM1 calculations[27] were performed[28] (for details, see the supplementary information) with the MOPAC algorithm implemented in the Cache 5.0 program package.[29] The structures chosen for these calculations were generated with 3000 step Monte Carlo conformational searches of favorable conformations with the Amber* force field implemented in MacroModel 8.0.[30] Generally, the force-field calculations and the AM1 results are in good agreement with each other so that we can concentrate on the AM1 calculations.

Rotaxanes **1@5** and **1@6** and their deprotonated analogues **1**$^-$**@5** and **1**$^-$**@6** were optimized in different conformations with a maximum number of hydrogen bonds (see Fig. 9 and the supplementary information). Three low-energy conformations were identified for **1@5** (type I to III in Fig. 9, top row). In the most favorable structure, the wheel is bound to the two carbonyl groups attached to one of the two ethylene diamine spacers. The wheel is located on one of the arms close to a stopper, and remote from the axle centerpiece. The second best conformer, which is higher in energy by *ca.* 14 kJ mol^{-1} bears the wheel hydrogen bonded to the two carbonyl groups of the isophthalic dicarboxamide centerpiece of the axle. The third structure is about 20 kJ mol^{-1} higher in energy than the first one. Here, hydrogen bonding again connects the amide NH hydrogens of the wheel with the two carbonyl groups of one of the axle side chains. The difference between the structures I and III can best be explained using Fig. 6 (top). In the type I structure the wheel is located on the axle branch with the amide group in its in conformation. This is the structure found in the crystal. In the type III structure, the wheel is however shifted towards the other branch of the axle which is connected to the central phenolate by the out amide group. Consequently, the calculations confirm in excellent agreement with the crystal structure§ and the NMR data that the wheel of the neutral rotaxane **1@5** is likely drawn towards one of the stoppers and is shifted away from the axle centerpiece.

Three low-energy conformations have also been found for the deprotonated rotaxane **1**$^-$**@5** which are within 5 kJ mol^{-1} in energy. In the lowest energy structure, the wheel is located at the center of the axle (type I in Fig. 9, middle row). Two hydrogen bonds are formed between the wheel and the phenolate, two additional hydrogen bonds between the second half of the wheel and one of the carbonyl groups adjacent to the central phenolate. The type II structure corresponds to the wheel binding to the phenolate and the more distant carbonyl group by a total of four hydrogen bonds. Finally, the wheel is located on one of the arms of the axle the in the third structure (type III). This third structure is analogous to the most favorable geometry of the protonated form. The NOE experiments discussed above strongly disagree with the calculations for the anionic rotaxane

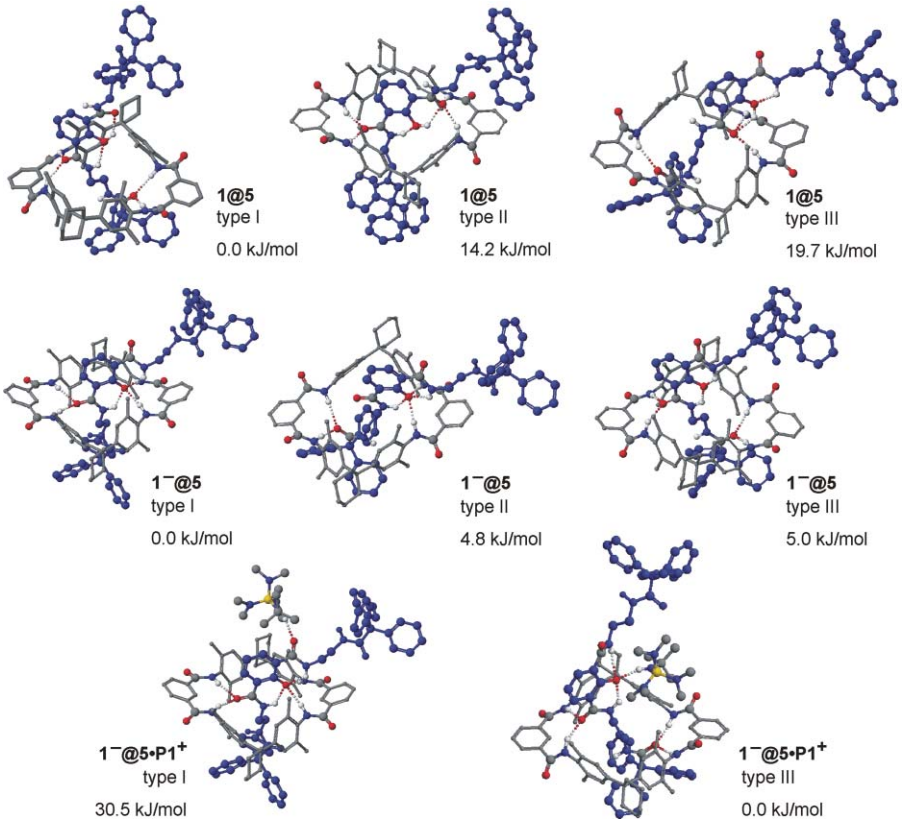

Fig. 9 Top: three low-energy conformations of **1**@**5**. Center: three energetically favorable conformations of the corresponding anion **1**$^-$@**5**. Bottom: two conformations of the complex of deprotonated rotaxane and P1 cation **1**$^-$@**5**·P1$^+$ revealing the importance of a close contact between cation and anion.

alone, *i.e.* without counterion and solvents. Instead, the presence of the counterion in close proximity of the axle is supported by the observation of NOE contacts between the P1 cation and the axle. Consequently, several conformations of the rotaxane were re-optimized with the counterion as close to the axle center piece as possible. These calculations provide a result which is in excellent agreement with the NOE contacts derived from the NMR experiments discussed above. A rotaxane conformation (type III) with the wheel shifted to one side of the axle and the cation in direct contact with the phenolate maximizes the electrostatic interactions and thus is energetically most favorable (Fig. 9, bottom row). Any conformation bearing the wheel hydrogen bonded to the central phenolate makes this close contact between the two charges impossible and renders these conformations energetically less favorable. One example which is less favorable by *ca.* 30 kJ mol^{-1} is shown in Fig. 9 (type I). Consequently, the calculations predict that the wheel position should remain the same independent of the protonation state. They also reveal that it is mandatory to take into account the counterion effects.

Since the calculations have been performed for isolated species without the surrounding solvent, electrostatic interactions between the P1 cation and the phenolate are likely overestimated as compared to the situation in solution, where they are reduced by the dielectricity constant of the solvent. As a consequence, the energy difference between the two conformations shown for **1**$^-$@**5**·P1$^+$ will be lower in the real system. If solvation of the cation is strong enough to generate free ions rather than ion pairs, the wheel might still not move to the central phenolate. The energy differences between type I–III structures of the deprotonated rotaxane are rather small. Although the calculations predict a slight preference for the wheel to shift towards the phenolate, solvent effects need to be taken into account. Close to the anion, one can expect to find stronger interactions of solvent molecules and rotaxane than in more remote positions so that the energies will further be biased in favor of the structure found in the NMR experiments. The wheel will reside close to the stoppers and not switch to the phenolate, if this assumption holds true.

Finally, the pyridine wheel **6** behaves quite similarly so that we shall refrain from an in-depth discussion of the rotaxanes **1**@**6** and **1**$^-$@**6** here. It should, however, be mentioned that the energy differences are small (*ca.* 6 kJ mol^{-1}) between structures with the pyridine close to the central phenol and those where the pyridine is bound to the carbonyl group adjacent to the stoppers. These calculations provide a rationalization for the finding of two different structures in a 1 : 3 ratio in the ^{1}H NMR spectra of **1**@**4**. It turns out that all structures (with one exception) maximizing the distance between the phenol and the pyridine nitrogen are slightly more favorable and we thus tentatively assign this arrangement to the set of more intense signals in the NMR spectrum shown in Fig. 5.

3. Dynamic properties: shuttling and rotary motions

An analysis of the dynamic properties must take into account several different motions. The first one is shuttling of the wheel along the axle. In principle, axle **1** offers three diamide stations to wheel **2** in the protonated form of the rotaxane. Two are located close to the stoppers separated by the two ethylene diamine moieties. The third one is the hydroxy isophthaloylamide in the axle center. Since NMR experiments, the crystal structure, and calculations agree with each other that the wheel is more favorably bound to one of the peripheral stations, one expects to observe a *degenerate shuttling motion* between the two ends of the axle. The second motion is the rotation of the wheel around the axle which likely superimposes the shuttling motion. Both motions can be expected to be affected by the protonation state of the axle center piece. Thus, both states need to be examined with respect to their dynamic features.

A first approach to these properties are temperature dependent NMR experiments. At 233 K, **1**@**2** and **1**$^-$@**2** in CD_2Cl_2 as well as DMF-d_7 exhibit two sets of signals for both the axle and the wheel. This indicates that both motions, shuttling and wheel rotation, are slow processes compared to the NMR timescale. Consequently, we have extended this NMR study to the temperature range between 223 and 293 K in both solvents. Not unexpectedly, the spectral changes are complex and thus we discuss here the most clear-cut case only.

The temperature dependent ^{1}H NMR spectra for deprotonated rotaxane **1**$^-$@**2** in dichloromethane are depicted in Fig. 10. If one follows the two wheel NH signals from the bottom spectrum to the top (dashed lines), it becomes clear that they coalesce at a temperature of $T_c = 278 \pm 2$ K and form one broad signal above that temperature. This coalescence is related to the circumrotation of the wheel around the axle which leads to fast exchange of the two sides of the wheel at higher temperatures. From the measurements, a barrier of *ca.* $\Delta G^{\ddagger} = 54 \pm 2$ kJ mol^{-1} can be calculated for this motion. This can be further verified by another pair of signals that also exhibits coalescence due to the same dynamic process: The two CH protons of the wheel's isophthalic acid units adjacent to the two amide groups (dotted lines) fall together in one signal at $T_c = 269 \pm 2$ K. At 293 K this signal has already sharpened significantly. Again, the barrier can be determined and amounts to *ca.* $\Delta G^{\ddagger} = 54 \pm 2$ kJ mol^{-1}. This barrier has been confirmed by EXSY experiments (57 ± 2 kJ mol^{-1}).

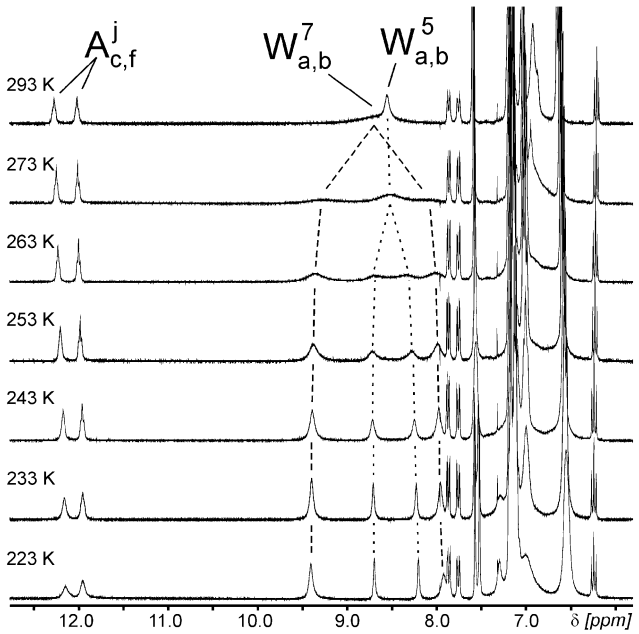

Fig. 10 Temperature-dependent ^{1}H NMR spectra (aromatic and NH regions) of **1**$^-$@**2** in CD_2Cl_2. Coalescence is observed at $T_c = 278 \pm 2$ K for $W^{7a,b}$ (dashed lines) and at $T_c = 269 \pm 2$ K for $W^{5a,b}$ (dotted lines). Note that the axle's NH signals ($A^j_{c,f}$) remain unaffected even at higher temperatures.

Since the two signals of the axle's two amide protons at around 12 ppm do not coalesce even at 293 K, the shuttling motion must have a higher activation barrier and is therefore considerably slower than rotation of the wheel. Consequently, it suffers from a significant steric barrier beyond mere cleavage of hydrogen bonds. While the circumrotation around the thin, thread-like ethylene diamine spacer groups can easily proceed through dissociation of all four hydrogen bonds in the absence of significant steric barriers, the phenol axle center piece appears to be a steric obstacle on the way of the wheel when traveling along the axle. This aspect can be related to our previous deslippage experiments, in which the aspect of steric size of stopper groups was closely examined.[10] In these experiments, it turned out that the tetralactam wheel passes over a 3,5-di-*t*-butyl phenyl stopper with a half life of *ca.* 60 h at 333 K. In our rotaxanes, the axle center piece does not have the large *t*-butyl groups, and thus the barrier is lower and the shuttling reaction faster than the deslipping reaction examined before.

Table 2 Rate constants k of the shuttling motion of **1**$^-$@**2** at 233 K. The values were derived from ^{1}H,^{1}H EXSY spectra using different solvent mixtures

Solvent mixtures	$k \times 10^{-2}$/s^{-1} [a]
CD_2Cl_2	5.1
CD_2Cl_2 + 10% DMSO-d_6	7.0
CD_2Cl_2 + 20% DMSO-d_6	10.4
CD_2Cl_2 + 40% DMSO-d_6	10.5
DMF-d_7	10.9
DMF-d_7 + 20% DMSO-d_6	9.1
DMF-d_7 + 40% DMSO-d_6	8.8
DMF-d_7 + 60% DMSO-d_6	9.8

[a] Error range $\pm 0.5 \times 10^{-2}$/s^{-1}.

To determine the dynamic behavior of movements being slow on the NMR time scale, also two dimensional EXSY spectra can be used.[31] In addition to the better signal dispersion of the exchange signals in the two dimensional spectra, also slow exchange rates can be determined from the integrals of the respective diagonal signals, exchange cross signals and the mixing time. This makes it possible to determine the shuttling rate of the wheel along the axle by EXSY NMR experiments. For the determination of the exchange rates, the proton signals ($A^h_{c,f}$ and $A^i_{c,f}$) of the ethylene spacers were chosen, since the wheel shuttling motion causes the largest chemical shift difference for these protons from the free to the occupied shuttling position (see above). To elucidate the influence of the solvent on the shuttling movement, EXSY spectra of **1**$^-$@**2** were recorded in dichloromethane-d_2, in DMF-d_7, in mixtures of dichloromethane-d_2 with increasing amounts of DMSO-d_6, and in mixtures of DMF-d_7 with increasing amounts of DMSO-d_6. The respective rate constants are given in Table 2.

The slowest shuttling rate of **1**$^-$@**2** is observed in pure CD_2Cl_2. The addition of 10% DMSO-d_6 leads to a significant increase of the shuttling rate by 40%, the addition of 20% DMSO-d_6, even to a doubling of the shuttling rate (experimental error: $\pm$10%). Since further addition of DMSO-d_6 does not lead to a further increase of the rate constant, a plateau for the shuttling rate appears to be reached. In pure DMF-d_7, the rate constant for the shuttling starts already at the plateau value of *ca.* 0.1 s^{-1}. Increasing amounts of DMSO-d_6 do not significantly affect the rate constants.

Now the question arises, whether these solvent effects can be explained by structural aspects. The NOE studies together with the theoretical calculations discussed above showed that the electrostatic interaction between the phenolate moiety and the P1 cation contributes to the displacement of the wheel from the "phenolate station". From the most favorable structure of **1**$^-$@**2**·P1 in Fig. 9, it becomes clear that the cation–phenolate interactions will hinder the shuttling movement: the stronger the electrostatic interactions between the counterions the stronger the effect of the "cation brake". Thus, in apolar solvents, the brake should work best. The more DMSO is added (which solvates the cation and lowers the electrostatic interactions) the faster the shuttling becomes. At a distinct amount of solvation, the shuttling speed reaches a plateau value, it is not further influenced by the cation brake.

This structural explanation can be directly confirmed by the experimentally derived rate constants and the corresponding NOE data. In pure CD_2Cl_2, the rate constant of **1**$^-$@**2** is at the lowest value and simultaneously NOE contacts of medium intensity are detected between the NH proton of the P1 cation

and protons of the axle as well as the wheel of the rotaxane. By addition of 10% DMSO-d_6 the rate constant increases. This is accompanied by reduced, but still detectable NOE contacts (Fig. 8 and 11). Starting from 20% DMSO-d_6, the NOE contacts to the base are below the detection limit (Fig. 11) and the rate constants reach their plateau value. In DMF-d_7, already the pure solvent solvates the base strongly enough to prevent NOE contacts as well as to induce rate constants on the plateau value. Although the solvation of the cation affects the shuttling movement, the structure and the preferred position of the wheel are not influenced by the use of different solvents. This is indicated by very similar chemical shifts of the protons of **1**$^-$@**2** in all these solvents. Interestingly, also protonated **1**@**2** shows a very similar plateau value of about 0.10 s^{-1} in mixtures of CD_2Cl_2 and DMSO-d_6.[32] In conclusion, the shuttling rate can be switched between a protonated fast-motion and a deprotonated slow-motion state in dichloromethane.

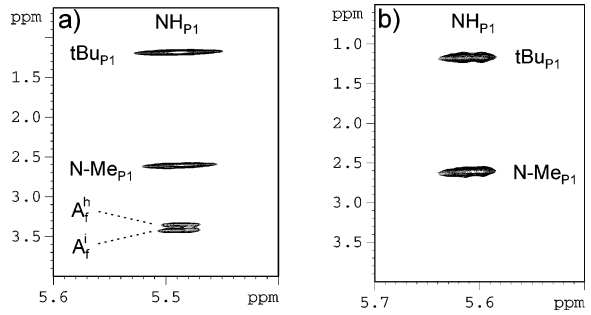

Fig. 11 Sections of ^{1}H,^{1}H NOESY spectra of **1**$^-$@**2** at 233 K in CD_2Cl_2 and 10% DMSO-d_6 (a) and in CD_2Cl_2 and 20% DMSO-d_6. (b) The vanishing of the dipolar interactions between the NH proton of the P1 base (NH_{P1}) and the ethylene protons of the uncovered half of the axle by adding further 10% of DMSO-d_6 exemplarily indicate the increased solvation of P1 by DMSO leading to reduced electrostatic interactions between P1 and the phenolate moiety.

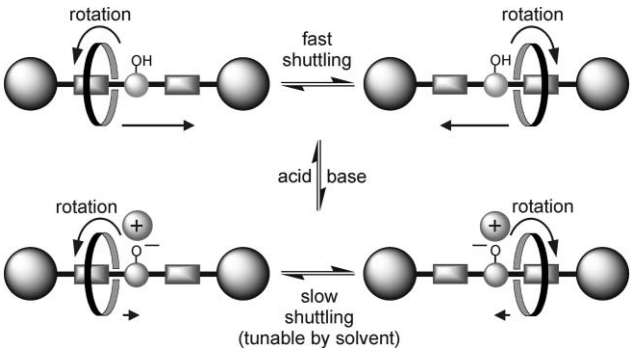

Fig. 12 Cartoon representation summarizing the dynamic processes involved in the acid/base controlled switching of rotaxanes **1**@**2**–**1**@**4**.

Conclusions

The rotaxanes under study were thoroughly characterized by NMR experiments, mass spectrometric methods, and crystal structure analysis. The phenolic OH group in the axle can also be employed to exert control over the dynamic properties of the rotaxane.

Based on a previous literature report,[12] switching of the preferred position of the wheel on the axle from one station to the other by the addition of acids and bases was expected. However, it turned out that the counterions and the solvent play a pivotal role for the control of the dynamic properties of the rotaxanes (Fig. 12). The wheel shuttling in the deprotonated rotaxanes is hampered by the counter-cation which is held by electrostatic forces in close proximity of the anion at the axle center piece. The "cation brake" described here does not completely suppress the shuttling motion, because the cation is bound by non-covalent forces and can reversibly dissociate, let the wheel pass over the phenolate, and reassociate subsequently. Consequently, the shuttling speed can be modulated for the first time by addition of acids and bases between a fast- and a slow-motion mode rather than switching it on and off. Depending on the solvent, the electrostatic interactions of cation and axle—and with them, the barrier for shuttling and its rate—can be fine tuned.

Modulating the speed through electrostatic interactions and tuning that modulation by the choice of solvent provide an interesting combination of complementary ways to adjust the dynamic features at will with high precision in the rotaxanes presented here. Although the effects found for the present system are still not very large, our system provides a proof-of-principle for the hypothesis that external stimuli can control the rate of molecular motions. In future, the effects may become larger through a fine-tuning of the axle structure modifying the steric barrier imposed by the central phenolate.

Acknowledgements

We are grateful to the Deutsche Forschungsgemeinschaft (DFG) and the Fonds der Chemischen Industrie (FCI) for financial support. PG acknowledges a postdoctoral fellowship from the Alexander-von-Humboldt foundation. CAS thanks the DFG for a Heisenberg fellowship and the FCI for a Dozenten-stipendium.

References and notes

1 For general reviews on template effects, see: D. H. Busch and N. A. Stephensen, *Coord. Chem. Rev.*, 1990, **100**, 119–154; R. Cacciapaglia and L. Mandolini, *Chem. Soc. Rev.*, 1993, **22**, 221–231; N. V. Gerbeleu, V. B. Arion and J. Burgess, *Template Synthesis of Macrocyclic Compounds*, Wiley-VCH, Weinheim, 1999; *Templated Organic Synthesis*, ed. F. Diederich and P. J. Stang, Wiley-VCH, Weinheim, 2000; T. J. Hubin and D. H. Busch, *Coord. Chem. Rev.*, 2000, **200**, 5–52.

2 For reviews on template effects for rotaxane and catenane synthesis, see: C. O. Dietrich-Buchecker and J.-P. Sauvage, *Chem. Rev.*, 1987, **87**, 795–810; J.-P. Sauvage, *Acc. Chem. Res.*, 1990, **23**, 319–327; S. Anderson, H. L. Anderson and J. K. M. Sanders, *Acc. Chem. Res.*, 1993, **26**, 469–475; R. Hoss and F. Vögtle, *Angew. Chem.*, 1994, **106**, 389–398; R. Hoss and F. Vögtle, *Angew. Chem., Int. Ed. Engl.*, 1994, **33**, 375–384; J.-C. Chambron, C. O. Dietrich-Buchecker, V. Heitz, J.-F. Nierengarten, J.-P. Sauvage, C. Pascard and J. Guilhem, *Pure Appl. Chem.*, 1995, **67**, 233–240; R. Jäger and F. Vögtle, *Angew. Chem.*, 1997, **109**, 966–980; R. Jäger and F. Vögtle, *Angew. Chem., Int. Ed. Engl.*, 1997, **36**, 930–944; S. A. Nepogodiev and J. F. Stoddart, *Chem. Rev.*, 1998, **98**, 1959–1976; F. M. Raymo and J. F. Stoddart, *Chem. Rev.*, 1999, **99**, 1043–1063; M. Kogej, P. Ghosh and C. A. Schalley, in *Strategies and Tactics in Organic Synthesis, vol. 4*, ed. M. Harmata, Elsevier, Amsterdam, 2004, pp. 171–210; P. Linnartz and C. A. Schalley, in *Encyclopedia of Supramolecular Chemistry*, ed. J. L. Atwood and J. W. Steed, Dekker, New York, 2004, 1194–1201; A. Rang and C. A. Schalley, *Catenanes and Interlinked Molecules*, ed. J. L. Atwood and J. W. Steed, 2004, 206–213.

3 Only a selection can be given here: C. O. Dietrich-Buchecker, J.-P. Sauvage and J.-M. Kern, *J. Am. Chem. Soc.*, 1984, **106**, 3043–3045; M. Cesario, C. O. Dietrich-Buchecker, A. Edel, J. Guilhem, J.-P. Kintzinger, C. Pascard and J.-P. Sauvage, *J. Am. Chem. Soc.*, 1986, **108**, 6250–6254; D. J. Cárdenas, A. Livoreil and J.-P. Sauvage, *J. Am. Chem. Soc.*, 1996, **118**, 11980–11981; F. Baumann, A. Livoreil, W. Kaim and J.-P. Sauvage, *Chem. Commun.*, 1997, 35–36; A. Livoreil, J.-P. Sauvage, N. Amaroli, V. Balzani, L. Flamigni and B. Ventura, *J. Am. Chem. Soc.*, 1997, **119**, 12114–12124; J.-C. Chambron, J.-P. Sauvage, K. Mislow, A. De Cian and J. Fischer, *Chem. Eur. J.*, 2001, **7**, 4085–4096; D. A. Leigh, P. J. Lusby, S. J. Teat, A. J. Wilson and J. K. Y. Wong, *Angew. Chem.*, 2001, **113**, 1586–1591; D. A. Leigh, P. J. Lusby, S. J. Teat, A. J. Wilson and J. K. Y. Wong, *Angew. Chem., Int. Ed.*, 2001, **40**, 1538–1543; P. Mobian, J.-M. Kern and J.-P. Sauvage, *J. Am. Chem. Soc.*, 2003, **125**, 2016–2017.

4 B. L. Allwood, N. Spencer, H. Shahriari-Zavareh, J. F. Stoddart and D. J. Williams, *J. Chem. Soc., Chem. Commun.*, 1987, 1064–1066; P. R. Ashton, I. Iriepa, M. V. Reddington, N. Spencer, A. M. Z. Slawin, J. F. Stoddart and D. J. Williams, *Tetrahedron Lett.*, 1994, **35**, 4835–4838; M. Asakawa, P. R. Ashton, S. E. Boyd, C. L. Brown, S.

Menzer, D. Pasini, J. F. Stoddart, M. S. Tolley, A. J. P. White, D. J. Williams and P. G. Wyatt, *Chem. Eur. J.*, 1997, **3**, 463–481.

5 A. G. Kolchinski, D. H. Busch and N. W. Alcock, *J. Chem. Soc., Chem. Commun.*, 1995, 1289–1291; P. R. Ashton, P. J. Campbell, E. J. T. Chrystal, P. T. Glink, S. Menzer, D. Philp, N. Spencer, J. F. Stoddart, P. A. Tasker and D. J. Williams, *Angew. Chem.*, 1995, **107**, 1997–2001; P. R. Ashton, P. J. Campbell, E. J. T. Chrystal, P. T. Glink, S. Menzer, D. Philp, N. Spencer, J. F. Stoddart, P. A. Tasker and D. J. Williams, *Angew. Chem., Int. Ed.*, 1995, **34**, 1865–1869; P. R. Ashton, E. J. T. Chrystal, P. T. Glink, S. Menzer, C. Schiavo, J. F. Stoddart, P. A. Tasker and D. J. Williams, *Angew. Chem.*, 1995, **107**, 2001–2004; P. R. Ashton, E. J. T. Chrystal, P. T. Glink, S. Menzer, C. Schiavo, J. F. Stoddart, P. A. Tasker and D. J. Williams, *Angew. Chem., Int. Ed.*, 1995, **34**, 1869–1871; P. T. Glink, C. Schiavo, J. F. Stoddart and D. J. Williams, *J. Chem. Soc., Chem. Commun.*, 1996, 1483–1490; P. R. Ashton, A. N. Collins, M. C. T. Fyfe, S. Menzer, J. F. Stoddart and D. J. Williams, *Angew. Chem.*, 1997, **109**, 760; P. R. Ashton, A. N. Collins, M. C. T. Fyfe, S. Menzer, J. F. Stoddart and D. J. Williams, *Angew. Chem., Int. Ed.*, 1997, **36**, 735–739; F. G. Gatti, D. A. Leigh, S. A. Nepogodiev, A. M. Z. Slawin, S. J. Teat and J. K. Y. Wong, *J. Am. Chem. Soc.*, 2001, **123**, 5983–5989.

6 F. Vögtle, S. Meier and R. Hoss, *Angew. Chem.*, 1992, **104**, 1628–1631; F. Vögtle, S. Meier and R. Hoss, *Angew. Chem., Int. Ed.*, 1992, **31**, 1619–1622; S. Ottens-Hildebrandt, S. Meier, W. Schmidt and F. Vögtle, *Angew. Chem.*, 1994, **106**, 1818–1821; S. Ottens-Hildebrandt, S. Meier, W. Schmidt and F. Vögtle, *Angew. Chem., Int. Ed.*, 1994, **33**, 1767–1770; S. Ottens-Hildebrandt, M. Nieger, K. Rissanen, J. Rouvinen, S. Meier, G. Harder and F. Vögtle, *J. Chem. Soc., Chem. Commun.*, 1995, 777–778; H. Adams, F. J. Carver and C. A. Hunter, *J. Chem. Soc., Chem. Commun.*, 1995, 809–810; A. G. Johnston, D. A. Leigh, R. J. Pritchard and M. D. Deegan, *Angew. Chem.*, 1995, **107**, 1324–1327; A. G. Johnston, D. A. Leigh, R. J. Pritchard and M. D. Deegan, *Angew. Chem., Int. Ed.*, 1995, **34**, 1209–1212; Y. Geerts, D. Muscat and K. Müllen, *Macromol. Chem. Phys.*, 1995, **196**, 3425–3435; D. A. Leigh, K. Moody, J. P. Smart, K. J. Watson and A. M. Z. Slawin, *Angew. Chem.*, 1996, **108**, 326–331; D. A. Leigh, K. Moody, J. P. Smart, K. J. Watson and A. M. Z. Slawin, *Angew. Chem., Int. Ed.*, 1996, **35**, 306–310; D. Muscat, A. Witte, W. Köhler, K. Müllen and Y. Geerts, *Macromol. Rapid Commun.*, 1997, **18**, 233–241; T. Dünnwald, A. H. Parham and F. Vögtle, *Synthesis*, 1998, **3**, 339–348; T. Schmidt, R. Schmieder, W. M. Müller, B. Kiupel and F. Vögtle, *Eur. J. Org. Chem.*, 1998, 2003–2007; A. H. Parham, R. Schmieder and F. Vögtle, *SYNLETT*, 1999, **12**, 1887–1890.

7 G. M. Hübner, J. Gläser, C. Seel and F. Vögtle, *Angew. Chem.*, 1999, **111**, 395–398; G. M. Hübner, J. Gläser, C. Seel and F. Vögtle, *Angew. Chem., Int. Ed.*, 1999, **38**, 383–386; C. Reuter, W. Wienand, G. M. Hübner, C. Seel and F. Vögtle, *Chem. Eur. J.*, 1999, **5**, 2692–2697; C. Reuter and F. Vögtle, *Org. Lett.*, 2000, **2**, 593–595; G. M. Hübner, C. Reuter, C. Seel and F. Vögtle, *Synthesis*, 2000, **1**, 103–108; C. Seel and F. Vögtle, *Chem. Eur. J.*, 2000, **6**, 21–24; C. A. Schalley, G. Silva, C. F. Nising and P. Linnartz, *Helv. Chim. Acta*, 2002, **85**, 1578–1596; X. Li, J. Illigen, M. Nieger, S. Michel and C. A. Schalley, *Chem. Eur. J.*, 2003, **9**, 1332–1347; J. A. Wisner, P. D. Beer, N. G. Berry and B. Tomapatanaget, *Proc. Natl. Acad. Sci. U. S. A.*, 2002, **99**, 4983–4986; J. A. Wisner, P. D. Beer, M. G. B. Drew and M. R. Sambrook, *J. Am. Chem. Soc.*, 2002, **124**, 12469–12476; M. A. Sambrook, P. D. Beer, J. A. Wisner, R. L. Paul and A. R. Cowley, *J. Am. Chem. Soc.*, 2004, **126**, 15364–15365.

8 (*a*) G. Schill, *Catenanes, Rotaxanes and Knots*, Academic Press, New York, 1971; (*b*) *Molecular Catenanes, Rotaxanes, and Knots*, ed. J.-P. Sauvage and C. Dietrich-Buchecker, Wiley-VCH, Weinheim, 1999.

9 For reviews on a variety of different molecular devices, see: (*a*) K. E. Drexler, *Annu. Rev. Biophys. Biomol. Struct.*, 1994, **23**, 377–405; Z. Asfari and J. Vicens, *J. Inclusion Phenom. Macrocyclic. Chem.*, 2000, **36**, 103–118; V. Balzani, A. Credi, F. M. Raymo and J. F. Stoddart, *Angew. Chem.*, 2000, **112**, 3484–3530; V. Balzani, A. Credi, F. M. Raymo and J. F. Stoddart, *Angew. Chem., Int. Ed.*, 2000, **39**, 3348–3391; B. L. Feringa, *Acc. Chem. Res.*, 2001, **34**, 504–513; T. R. Kelly, *Acc. Chem. Res.*, 2001, **34**, 514–522; C. A. Schalley, *Angew. Chem.*, 2002, **114**, 1583–1586; C. A. Schalley, *Angew. Chem., Int. Ed.*, 2002, **41**, 1513–1515; V. Balzani, M. Venturi, A. Credi, *Molecular Devices and Machines: A Journey into the Nanoworld*, Wiley-VCH, Weinheim, 2003; C. A. Schalley, A. Lützen and M. Albrecht, *Chem. Eur. J.*, 2004, **10**, 1072–1080.

10 For studies on the stability of rotaxanes, see: H. W. Gibson, S. Liu, P. Lecavalier, C. Wu and Y. X. Shen, *J. Am. Chem. Soc.*, 1995, **117**, 852–874; F. M. Raymo, K. N. Houk and J. F. Stoddart, *J. Am. Chem. Soc.*, 1998, **120**, 9318–9322; G. Hübner, G. Nachtsheim, Q.-Y. Li, C. Seel and F. Vögtle, *Angew. Chem.*, 2000, **112**, 1315–1318; G. Hübner, G. Nachtsheim, Q.-Y. Li, C. Seel and F. Vögtle, *Angew. Chem., Int. Ed.*, 2000, **39**, 1269–1272; C. Heim, A. Affeld, M. Nieger and F. Vögtle, *Helv. Chim. Acta*, 1999, **82**, 746–759; A. Affeld, G. M. Hübner, C. Seel and C. A. Schalley, *Eur. J. Org. Chem.*, 2001, 2877–2890; T. Felder and C. A. Schalley, *Angew. Chem.*, 2003, **115**, 2360–2363; T. Felder and C. A. Schalley, *Angew. Chem., Int. Ed.*, 2003, **42**, 2258–2260; P. Linnartz and C. A. Schalley, *Supramol. Chem.*, 2004, 263–267.

11 J.-C. Chambron, S. Chardon-Noblat, A. Harriman, V. Heitz and J.-P. Sauvage, *Pure Appl. Chem.*, 1993, **65**, 2343–2349; A. C. Benniston, *Chem. Soc. Rev.*, 1996, **25**, 427–436; V. Balzani, M. Gómez-López and J. F. Stoddart, *Acc. Chem. Res.*, 1998, **31**, 405–413; J.-P. Sauvage, *Acc. Chem. Res.*, 1998, **31**, 611–619; J.-P. Collin, P. Gaviña, V. Heitz and J.-P. Sauvage, *Eur. J. Inorg. Chem.*, 1998, 1–14; R. Ballardini, V. Balzani, A. Credi, M. T. Gandolfi and M. Venturi, *Acc. Chem. Res.*, 2001, **34**, 445–455; C. A. Schalley, K. Beizai and F. Vögtle, *Acc. Chem. Res.*, 2001, **34**, 465–476; J.-P. Collin, C. Dietrich-Buchecker, P. Gaviña, M. C. Jimenez-Molero and J.-P. Sauvage, *Acc. Chem. Res.*, 2001, **34**, 477–487; T. Felder and C. A. Schalley, in *Highlights in Bioorganic Chemistry*, ed. C. Schmuck and H. Wennemers, Wiley-VCH, Weinheim, 2004, pp. 526–539; C. A. Schalley, *J. Phys. Org. Chem.*, 2004, **17**, 967–972.

12 R. A. Bissell, E. Córdova, A. E. Kaifer and J. F. Stoddart, *Nature*, 1994, **369**, 133–137; C. M. Keaveney and D. A. Leigh, *Angew. Chem.*, 2004, **116**, 1242–1244; C. M. Keaveney and D. A. Leigh, *Angew. Chem., Int. Ed.*, 2004, **43**, 1222–1224.

13 P. R. Ashton, R. Ballardini, V. Balzani, A. Credi, K. R. Dress, E. Ishow, C. J. Kleverlaan, O. Kocian, J. A. Preece, N. Spencer, J. F. Stoddart, M. Venturi and S. A. Wenger, *Chem. Eur. J.*, 2000, **6**, 3558–3574; A. M. Brouwer, C. Frochot, F. G. Gatti, D. A. Leigh, L. Mottier, F. Paolucci, S. Roffia and G. W. H. Wurpel, *Science*, 2001, **291**, 2124–2128.

14 A. Altieri, F. G. Gatti, E. R. Kay, D. A. Leigh, F. Paolucci, A. M. Z. Slawin and J. K. Y. Wong, *J. Am. Chem. Soc.*, 2003, **125**, 8644–8654.

15 D. J. Cárdenas, P. Gaviñas and J.-P. Sauvage, *Chem. Commun.*, 1996, 1915–1916; D. B. Amabilino, C. O. Dietrich-Buchecker and J.-P. Sauvage, *J. Am. Chem. Soc.*, 1996, **118**, 3285–3286; D. J. Cárdenas, P. Gaviñas and J.-P. Sauvage, *J. Am. Chem. Soc.*, 1997, **119**, 2656–2664.

16 F. Diederich, L. Echegoyen, M. Gómez-López, R. Kessinger and J. F. Stoddart, *J. Chem. Soc., Perkin Trans. 2*, 1999, 1577–1586.

17 F. Vögtle, W. M. Müller, U. Müller, M. Bauer and K. Rissanen, *Angew. Chem.*, 1993, **105**, 1356–1358; F. Vögtle, W. M. Müller, U. Müller, M. Bauer and K. Rissanen, *Angew. Chem., Int. Ed. Engl.*, 1993, **32**, 1295–1297.

18 S. S. Zhu, P. J. Carroll and T. M. Swager, *J. Am. Chem. Soc.*, 1996, **118**, 8713–8714.

19 A. Credi, V. Balzani, S. J. Langford and J. F. Stoddart, *J. Am. Chem. Soc.*, 1997, **119**, 2679–2681; M. Asakawa, P. R. Ashton, V. Balzani, A. Credi, G. Mattersteig, O. A. Matthews, M. Montalti, N. Spencer, J. F. Stoddart and M. Venturi, *Chem. Eur. J.*, 1997, **3**, 1992–1996.

20 P. Ghosh, O. Mermagen and C. A. Schalley, *Chem. Commun*, 2002, 2628–2629.

21 C. A. Hunter, *J. Chem. Soc., Chem. Commun.*, 1991, 749–751; C. A. Hunter, *J. Am. Chem. Soc.*, 1992, **114**, 5303–5311.

22 C. Seel, A. H. Parham, O. Safarowsky, G. M. Hübner and F. Vögtle, *J. Org. Chem.*, 1999, **64**, 7236–7242.

23 Examples of rotaxanes, in which the shuttling motion could be altered through different axle lengths: S. S. Kang, S. A. Vignon, H. R. Tseng and J. F. Stoddart, *Chem. Eur. J.*, 2004, **10**, 2555–2564; through implementation of different functional or blocking groups in the axle:; A. S. Lane, D. A. Leigh and A. Murphy, *J. Am. Chem. Soc.*, 1997, **119**, 11092–11093; M. Bélohradsky, A. M. Elizarov and J. F. Stoddart, *Collect. Czech. Chem. Commun.*, 2002, **11**, 1719–1728; J. O. Jeppensen, J. Becher and J. F. Stoddart, *Org. Lett.*, 2002, **4**, 557–560; J. O. Jeppensen, K. A. Nielsen, J. Perkins, S. A. Vignon, A. DiFabio, R. Ballardini, M. T. Gandolfi, M. Venturi, V. Balzani, J. Becher and J. F. Stoddart, *Chem. Eur. J.*, 2003, **9**, 2982–3007; through addition of different solvents:; D. B. Amabilino, P. R. Ashton, V. Balzani, C. L. Brown, A. Credi, J. M. J. Frechet, J.W. Leon, F. M. Raymo, N. Spencer, J. F. Stoddart and M. Venturi, *J. Am. Chem. Soc.*, 1996, **48**, 12012–12020; J. G. Cao, M. C. T. Fyfe, J. F. Stoddart, G. R. L. Cousins and P. T. Glink, *J. Org. Chem.*, 2000, **7**, 1937–1946; through dimerization of rotaxanes at the axle center:; L. Jiang, J. Okano, A. Orita and J. Otera, *Angew. Chem.*, 2004, **116**, 2173–2176; L. Jiang, J. Okano, A. Orita and J. Otera, *Angew. Chem., Int. Ed.*, 2004, **43**, 2121–2124.

24 For recent reviews of the mass spectrometric analysis of supramolecular species, see: C. A. Schalley, *Int. J. Mass Spectrom.*, 2000, **194**, 11–39; C. A. Schalley, *Mass Spectrom. Rev.*, 2001, **20**, 253–309.

25 For a more detailed study on the negative on ESI mass spectra of tetralactam macrocycles, catenanes, and rotaxanes, see: C. A. Schalley, J. Hoernschemeyer, X. Li, G. Silva and P. Weis, *Int. J. Mass*

Spectrom., 2003, **228**, 373–388; C. A. Schalley, P. Ghosh and M. Engeser, *Int. J. Mass Spectrom.*, 2004, **232**, 249–258.
26 R. Schwesinger, C. Hasenfratz, H. Schlemper, L. Walz, E.-M. Peters, K. Peters and H. G. von Schnering, *Angew. Chem.*, 1993, **105**, 1420–1422; R. Schwesinger, C. Hasenfratz, H. Schlemper, L. Walz, E.-M. Peters, K. Peters and H. G. von Schnering, *Angew. Chem., Int. Ed.*, 1993, **32**, 1361–1363.
27 M. J. S. Dewar, E. G. Zoebisch, E. F. Healy and J. J. P. Stewart, *J. Am. Chem. Soc.*, 1985, **107**, 3902–3209.
28 A validation of the AM1 semi-empirical method for the species under study was performed earlier: W. Reckien and S. Peyerimhoff, *J. Phys. Chem. A*, 2003, **107**, 9634; P. Linnartz, S. Bitter and C. A. Schalley, *Eur. J. Org. Chem.*, 2003, 4819; C. A. Schalley, W. Reckien, S. Peyerimhoff, B. Baytekin and F. Vögtle, *Chem. Eur. J.*, 2004, **10**, 4777–4789. In the latter reference, calculations are included which take into account solvent effects.
29 *CACHE 5.0 for Windows*, Fujitsu Ltd. 2001, Krakow, Poland.
30 Schrödinger, Inc. 1500 SW First Avenue, Suite 1180, Portland, OR 97201, USA. Also, see: F. Mohamadi, N. G. Richards, W. C. Guida, R. Liskamp, C. Caulfield, G. Chang, T. Hendrickson and W. C. Still, *J. Comput. Chem.*, 1990, **11**, 440; D. Q. McDonald and W. C. Still, *Tetrahedron Lett.*, 1992, **33**, 7743–7746.
31 H. Günther, *NMR-Spektroskopie, 3rd ed.*, Thieme, Stuttgart: 1992, pp. 314–317.
32 It should be noted that the poorer solubility of the neutral rotaxane limits the range of solvent mixtures available for these experiments.